L-3,4-Dihydroxy-6-[18F]fluorophenylalanine [18F]FDOPA

Created: March 21, 2005
Updated: May 19, 2005

Chemical name: L-3,4-Dihydroxy-6-[18F] fluorophenylalanine
Abbreviated name: 6-[18F]Fluoro-L-DOPA, [18F] FDOPA, FDOPA
Synonym:
Backbone: Amino acid
Targets: Aromatic L-amino acid decarboxylase; L-type amino acid transporter system
Mechanism: Uptake and decarboxylation
Method of detection: PET
Source of signal: 18F
Activation: No
***In vitro* studies:** Yes
Rodent studies: Yes
Other non-primate mammal studies: Yes
Non-human primate studies: Yes
Human studies: Yes

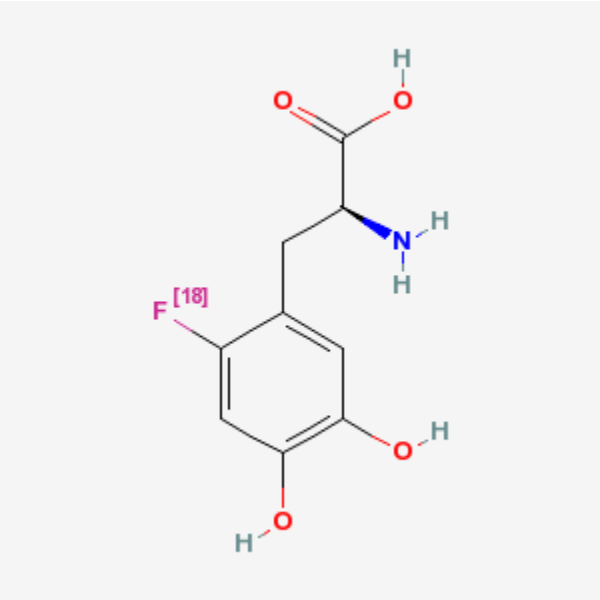

Click on the above structure for additional information in PubChem [http://pubchem.ncbi.nlm.nih.gov/].

Background

[PubMed]

Parkinson's disease (PD) is associated with a loss of dopamine-containing neurons in the striatum of the brain (1, 2). PD is caused by a shortage of dopamine. Dopamine, a neurotransmitter, plays an important role in the mediation of movement, cognition, and emotion. Dopamine also plays a role in various neuropsychiatric disorders, such as schizophrenia, autism, attention deficit hyperactivity disorder, and drug abuse.

Dopamine is synthesized within nerve cells (3). L-Tyrosine is converted to dihydroxyphenylalanine (L-DOPA) and then to dopamine in a two-step process. The first, rate-limiting step is catalyzed by tyrosine 3-monooxygenase (tyrosine hydroxylase or TH). The second step is catalyzed by aromatic L-amino acid decarboxylase (L-DOPA decarboxylase, AAAD). In parts of the nervous system that release dopamine as a neurotransmitter (dopaminergic neurons), no further metabolism occurs, and dopamine is stored in vesicles in the presynaptic nerve terminals by virtue of the dopamine reuptake transporter, DAT.

6-[18F]Fluoro-L-DOPA (FDOPA) is a radiolabeled analog of L-DOPA used to evaluate the central dopaminergic function of presynaptic neurons using positron emission tomography (PET) (4, 5). FDOPA PET reflects DOPA transport into the neurons, DOPA decarboxylation, and dopamine storage capacity. The tracer is converted to 6-[18F]fluorodopamine (FDA) by AAAD and is retained in the striatum. FDA can be *O*-methylated by catechol-*O*-methyltransferase (COMT) to 3-*O*-methyl-6-[18F]fluoro-L-dopa (3-OMFD), which is uniformly distributed throughout the brain. FDA is also metabolized via monoamine oxidase to yield [18F]6-fluoro-3,4-dihydroxyphenylacetic acid (FDOPAC) and subsequently by COMT to yield [18F]6-fluorohomovanillic acid (FHVA). AAAD and COMT are also present in peripheral tissues such as liver, kidneys, and lung. In clinical studies, AAAD is commonly inhibited with carbidopa, whereas COMT is blocked by entacapone and nitecapone. The availability of FDOPA in the brain is enhanced by these two types of inhibitors.

Synthesis

[PubMed]

FDOPA can be synthesized by either electrophilic or nucleophilic process (6). Regioselective electrophilic fluorodemetallation of either a mercuryl or a trimethylstannyl precursor is rapid and simple. Electrophilic fluorination of L-methyl-*N*-acetyl-[methoxy-4-acetoxyphenyl]alanine with [18F] acetyl hypofluorite to provide FDOPA in 8% radiochemical yield at the end of bombardment after hydrolysis and high-performance liquid chromatography (HPLC) purification (7). An overall synthesis time is 100 min with a 95% chemical purity and a specific activity of 7.4 GBq/mmol (200 mCi/mmol) at the end of synthesis (EOS). A robotic synthesis was performed using [18F]F_2/neon gas and the trimethylstannyl precursor in about 110 min (8). The radiochemical purity was >97%, and the specific activity was 2.59 GBq/mmol (70 mCi/mmol) at the EOS. The radiochemical yield was about 8.2% (uncorrected for decay).

A multi-step synthesis, based on the nucleophilic displacement of a nitro group using the standard [18F] potassium Kryptofix complex, has been reported (9). The chemical purity was >96% with the specific activity of 37 GBq//μmol (1 Ci/μmol) at the EOS. The overall radiochemical yield was 23% at the EOS. The total synthesis time was 90 min. Nucleophilic methods using the [18F]fluoride ion have the potential to provide a higher yield and a higher specific activity.

In Vitro Studies: Testing in Cells and Tissues

[PubMed]

The enzyme kinetic parameters for AAAD of DOPA and FDOPA were determined *in vitro* (10). The K_m and k_{cat} for DOPA were 0.091 mM and 9.1 s^{-1}, respectively. The K_m and k_{cat} for FDOPA were 0.7 mM and 8.2 s^{-1}, respectively. The presence of fluorine at ring position 6 decreased binding to the active site of AAAD without significantly affecting the enzyme activity of AAAD.

Unlabeled FDOPA (50 μM) reduced [3H]L-DOPA (25 nM) uptake by 69% and 49% in rat striatal and cortical synaptosomes, respectively. L-DOPA showed a higher inhibition than FDOPA (11). In another study, 3-OMFD, L-DOPA, and unlabeled FDOPA inhibited the uptake of [3H]tryptophan (0.1μM) into cells transfected with human L-type amino acid transporter with IC_{50}s of 84, 46, and 878 μM, respectively (12).

Animal Studies

Rodents

[PubMed]

Biodistribution studies showed a high uptake of radioactivity in the kidneys (5.6% injected dose (ID)/organ), pancreas (0.9% ID/organ), and liver (0.7% ID/organ) of mice at 1 h after injection of FDOPA (13).

Total extracellular [18F] radioactivity in the rat striatum peaked at 30 min after injection of FDOPA and declined with a clearance half-life of 2 h (14). In the extracellular space, the dominant FDOPA metabolite at early times was FDOPAC, followed by FHVA at 50 min. F-sulfoconjugates appeared at 70 min, and finally 3-OMFD appeared later. Analysis of the striatal tissue confirmed the intra-neuronal localization of FDA, most likely stored in vesicles, slowing its cerebral clearance.

In the rat brain, carbidopa pretreatment increased striatal FDA (700%) and 3-OMFD (230%) at 30 min after injection of FDOPA and cerebellum FDA (370%) and 3-OMFD (300%) (15). FDOPA plasma levels increased by 20%, and 3-OMFD plasma levels increased by 220%. FDOPAC and FDA were not detected. FHVA levels (>5%) were not changed by carbidopa pretreatment. Carbidopa restricted peripheral FDOPA metabolism to 3-OMFD formation and increased FDOPA bioavailability to the brain, resulting in greater FDA accumulation in the striatum.

The uptake of FDOPA was studied in a rat model of PD (16). The brains of these rats were unilaterally lesioned with an intranigral injection of 6-hydroxydopamine. The uptake in the lesioned side was 16-31% lower than the sham controls and intact side of the striatum and substantia nigra. The uptake data correlated with the behavioral tests and the number of nigral dopaminergic neurons.

Other Non-Primate Mammals

[PubMed]

In dogs, FDOPA uptake was greatest in the pituitary, followed by the liver, spleen, and kidneys at 1 h after injection. The uptake in the brain cortex, striatum, thalamus, and cerebellum was <50% of the liver uptake (17).

FDOPA metabolism of immature brain was studied in newborn piglets (18). The estimated values of FDOPA decarboxylation in the basal ganglia were similar to values calculated in adult animals and humans. However, a significant FDOPA decarboxylation was also found in the frontal cortex and the cerebellum. HPLC analysis of brain samples also revealed extensive and rapid metabolism of FDOPA in the frontal cortex, caudate/putamen, midbrain, and cerebellum. At 8 min after tracer injection, about 80% of FDOPA was already converted to FDA and its metabolites. Surprisingly, a

rather high fraction (16-21%) of [18F]fluoro-3-methoxytyramine was found, indicating a low storage capacity of vesicular dopamine at this perinatal stage. In a later study, it was found that the metabolism of FDOPA in young pigs was significantly faster than in newborns (19).

Non-Human Primates

[PubMed]

FDOPA PET studies in non-human primates have provided useful assessments of the dopaminergic function in the brain. The major metabolite detected in the periphery was 3-OMFD (15). Carbidopa pretreatment increased FDOPA bioavailability to the brain and increased FDOPA metabolism to FDA and 3-OMFD. In the striatum, FDA and 3-OMFD were the major FDOPA metabolites, with lower levels of FDOPAC and FHVA. In contrast, the cerebellum and cortex had mainly FDOPA and 3-OMFD accumulation (20-22).

Carbidopa pretreatment of monkeys showed inhibition of peripheral decarboxylation of FDOPA and higher uptake in the striatum and cortex than the control monkeys (15). There was no change in the FDOPA influx constant. Therefore, the higher uptake was caused by higher FDOPA bioavailability for transport into the brain.

FDOPA metabolites from putamen of normal and 1-methyl-4-phenyl-1,2,3,6-tetrahydropyridine (MPTP)-treated monkeys were measured to correlate FDOPA metabolism with that of the endogenous dopamine system (23). There were less than 2% of control FDOPA and dopamine levels in the MPTP-treated putamen, which had 80% 3-OMFD as the major metabolite. FDA metabolism was increased for the lesioned putamen as measured by FHVA/FDA ratios (6:1 *vs.* 0.38:1). At 60 min after FDOPA injection, similar plasma activity for FDOPA and its metabolites were found for both control and lesioned monkeys. The results suggested that PET studies with FDOPA in PD patients could provide kinetic evaluation of striatal biochemistry and evidence of *in vivo* dopamine turnover changes.

Human Studies

[PubMed]

Human dosimetry was estimated based on murine and human biodistribution data (13, 17). The bladder wall receives the highest dose (0.215 mGy/MBq or 0.797 rad/mCi). Other organs receiving high doses are the kidneys (0.089 mGy/MBq or 0.329 rad/mCi) and pancreas (0.030 mGy/MBq or 0.110 rad/mCi). The brain, liver, and lungs receive <0.008 mGy/MBq (0.029 rad/mCi). An effective dose equivalent of 0.026 mSv/MBq (96 mrem/mCi) was estimated in the intravenous administration of FDOPA.

The first FDOPA PET study of human brain was reported in 1983 (24), showing the localization of radioactivity in the striatum. Only about 1% of FDOPA entered the brain. Striatal-to-occipital ratio, FDOPA influx constant, and the AAAD activity constant are commonly used as analytical parameters in FDOPA PET studies. In patients with established bilateral PD, FDOPA PET showed reductions of the bilateral influx constant in the caudate, putamen, striatal nigra, and midbrain

tegmentum. The decline in FDOPA uptake was more rapid in PD patients than in normal subjects (25). In PD patients, AAAD activity was reduced in striatum, putamen, and caudate and no change in frontal and occipital cortices (26).

In carbidopa-pretreated subjects, peripheral FDOPA was rapidly metabolized by COMT to 3-OMFD. There were significant increases in FDOPA plasma levels for 30 min, but the FHVA level decreased. Inhibition of COMT by entacapone in mild to moderate PD patients prolonged the circulation time of FDOPA in the plasma (27) but did not change the rate constants for striatal FDOPA influx or decarboxylation. In advanced PD patients pretreated with entacapone, the FDOPA influx constant decreased significantly in the caudate and putamen, and no change in healthy controls. This may be because of the advanced disease, decreased storage capacity, or both (28).

FDOPA PET permits objective monitoring of PD progression and neuroprotection therapies. It allows diagnosis of PD in early disease stages. In recent studies, FDOPA has also demonstrated its usefulness for imaging brain tumors (29) and neuroendocrine metastatic lesions in bone (30).

References

1. Carbon M, Ghilardi MF, Feigin A, Fukuda M, Silvestri G, Mentis MJ, Ghez C, Moeller JR, Eidelberg D. Learning networks in health and Parkinson's disease: reproducibility and treatment effects. Hum Brain Mapp 19:197–211; 2003. (PubMed)
2. Chesselet MF, Delfs JM. Basal ganglia and movement disorders: an update. Trends Neurosci 19:417–422; 1996. (PubMed)
3. Barrio JR, Huang SC, Phelps ME. Biological imaging and the molecular basis of dopaminergic diseases. Biochem Pharmacol 54:341–348; 1997. (PubMed)
4. Heiss WD, Hilker R. The sensitivity of 18-fluorodopa positron emission tomography and magnetic resonance imaging in Parkinson's disease. Eur J Neurol 11:5–12; 2004. (PubMed)
5. Thobois S, Guillouet S, Broussolle E. Contributions of PET and SPECT to the understanding of the pathophysiology of Parkinson's disease. Neurophysiol Clin 31:321–340; 2001. (PubMed)
6. Luxen A, Guillaume M, Melega WP, Pike VW, Solin O, Wagner R. Production of 6-[18F]fluoro-L-dopa and its metabolism in vivo--a critical review. Int J Rad Appl Instrum B 19:149–158; 1992. (PubMed)
7. Adam MJ, Ruth TJ, Grierson JR, Abeysekera B, Pate BD. Routine synthesis of L-[18F]6-fluorodopa with fluorine-18 acetyl hypofluorite. J Nucl Med 27:1462–1466; 1986. (PubMed)
8. Chang CW, Wang HE, Lin HM, Chtsai CS, Chen JB, Liu RS. Robotic synthesis of 6-[18F]fluoro-L-dopa. Nucl Med Commun 21:799–802; 2000. (PubMed)
9. Lemaire C, Damhaut P, Plenevaux A, Comar D. Enantioselective synthesis of 6-[fluorine-18]-fluoro-L-dopa from no-carrier-added fluorine-18-fluoride. J Nucl Med 35:1996–2002; 1994. (PubMed)
10. Borri Voltattorni C, Bertoldi M, Bianconi S, Deng WP, Wong K, Kim I, Herbert B, Kirk KL. Behavior of fluorinated analogs of L-(3,4-dihydroxyphenyl)alanine and L-threo-(3,4-dihydroxyphenyl)serine as substrates for Dopa decarboxylase. Biochem Biophys Res Commun 295:107–111; 2002. (PubMed)
11. Yee RE, Cheng DW, Huang SC, Namavari M, Satyamurthy N, Barrio JR. Blood-brain barrier and neuronal membrane transport of 6-[18F]fluoro-L-DOPA. Biochem Pharmacol 62:1409–1415; 2001. (PubMed)
12. Brust P, Vorwieger G, Walter B, Fuchtner F, Stark H, Kuwabara H, Herzau M, Opfermann T, Steinbach J, Ganapathy V, et al. The influx of neutral amino acids into the porcine brain during development: a positron emission tomography study. Brain Res Dev Brain Res 152:241–253; 2004. (PubMed)
13. Mejia AA, Nakamura T, Itoh M, Hatazawa J, Ishiwata K, Ido T, Matsumoto M, Watabe H, Watanuki S, Seo S. Absorbed dose estimates in positron emission tomography studies based on the administration of 18F-labeled radiopharmaceuticals. J Radiat Res (Tokyo) 32:243–261; 1991. (PubMed)

14. DeJesus OT, Haaparanta M, Solin O, Nickles RJ. 6-fluoroDOPA metabolism in rat striatum: time course of extracellular metabolites. Brain Res 877:31–36; 2000. (PubMed)

15. Melega WP, Hoffman JM, Luxen A, Nissenson CH, Phelps ME, Barrio JR. The effects of carbidopa on the metabolism of 6-[18F]fluoro-L-dopa in rats, monkeys and humans. Life Sci 47:149–157; 1990. (PubMed)

16. Forsback S, Niemi R, Marjamaki P, Eskola O, Bergman J, Gronroos T, Haaparanta M, Haapalinna A, Rinne J, Solin O. Uptake of 6-[18F]fluoro-L-dopa and [18F]CFT reflect nigral neuronal loss in a rat model of Parkinson's disease. Synapse 51:119–127; 2004. (PubMed)

17. Harvey J, Firnau G, Garnett ES. Estimation of the radiation dose in man due to 6-[18F]fluoro-L-dopa. J Nucl Med 26:931–935; 1985. (PubMed)

18. Brust P, Bauer R, Walter B, Bergmann R, Fuchtner F, Vorwieger G, Steinbach J, Johannsen B, Zwiener U. Simultaneous measurement of [18F]FDOPA metabolism and cerebral blood flow in newborn piglets. Int J Dev Neurosci 16:353–364; 1998. (PubMed)

19. Brust P, Walter B, Hinz R, Fuchtner F, Muller M, Steinbach J, Bauer R. Developmental changes in the activities of aromatic amino acid decarboxylase and catechol-O-methyl transferase in the porcine brain: a positron emission tomography study. Neurosci Lett 364:159–163; 2004. (PubMed)

20. Chan GL, Doudet DJ, Dobko T, Hewitt KA, Schofield P, Pate BD, Ruth TJ. Routes of administration and effect of carbidopa pretreatment on 6-[18F]fluoro-L-dopa/PET scans in non-human primates. Life Sci 56:1759–1766; 1995. (PubMed)

21. Endres CJ, DeJesus OT, Uno H, Doudet DJ, Nickles JR, Holden JE. Time profile of cerebral [18F]6-fluoro-L-DOPA metabolites in nonhuman primate: implications for the kinetics of therapeutic L-DOPA. Front Biosci 9:505–512; 2004. (PubMed)

22. Melega WP, Grafton ST, Huang SC, Satyamurthy N, Phelps ME, Barrio JR. L-6-[18F]fluoro-dopa metabolism in monkeys and humans: biochemical parameters for the formulation of tracer kinetic models with positron emission tomography. J Cereb Blood Flow Metab 11:890–897; 1991. (PubMed)

23. Melega WP, Hoffman JM, Schneider JS, Phelps ME, Barrio JR. 6-[18F]fluoro-L-dopa metabolism in MPTP-treated monkeys: assessment of tracer methodologies for positron emission tomography. Brain Res 543:271–276; 1991. (PubMed)

24. Garnett ES, Firnau G, Nahmias C. Dopamine visualized in the basal ganglia of living man. Nature 305:137–138; 1983. (PubMed)

25. Vingerhoets FJ, Snow BJ, Lee CS, Schulzer M, Mak E, Calne DB. Longitudinal fluorodopa positron emission tomographic studies of the evolution of idiopathic parkinsonism. Ann Neurol 36:759–764; 1994. (PubMed)

26. Kuwabara H, Cumming P, Yasuhara Y, Leger GC, Guttman M, Diksic M, Evans AC, Gjedde A. Regional striatal DOPA transport and decarboxylase activity in Parkinson's disease. J Nucl Med 36:1226–1231; 1995. (PubMed)

27. Ishikawa T, Dhawan V, Chaly T, Robeson W, Belakhlef A, Mandel F, Dahl R, Margouleff C, Eidelberg D. Fluorodopa positron emission tomography with an inhibitor of catechol-O-methyltransferase: effect of the plasma 3-O-methyldopa fraction on data analysis. J Cereb Blood Flow Metab 16:854–863; 1996. (PubMed)

28. Ruottinen HM, Rinne JO, Ruotsalainen UH, Bergman JR, Oikonen VJ, Haaparanta MT, Solin OH, Laihinen AO, Rinne UK. Striatal [18F]fluorodopa utilization after COMT inhibition with entacapone studied with PET in advanced Parkinson's disease. J Neural Transm Park Dis Dement Sect 10:91–106; 1995. (PubMed)

29. Becherer A, Karanikas G, Szabo M, Zettinig G, Asenbaum S, Marosi C, Henk C, Wunderbaldinger P, Czech T, Wadsak W, et al. Brain tumour imaging with PET: a comparison between [18F]fluorodopa and [11C] methionine. Eur J Nucl Med Mol Imaging 30:1561–1567; 2003. (PubMed)

30. Becherer A, Szabo M, Karanikas G, Wunderbaldinger P, Angelberger P, Raderer M, Kurtaran A, Dudczak R, Kletter K. Imaging of advanced neuroendocrine tumors with (18)F-FDOPA PET. J Nucl Med 45:1161–1167; 2004. (PubMed)